Reassessing the substrate specificities of the major *Staphylococcus aureus* peptidoglycan hydrolases lysostaphin and LytM

Lina Antenucci[1], Salla Virtanen[2], Chandan Thapa[1], Minne Jartti[1,#], Ilona Pitkänen[1], Helena Tossavainen[1], Perttu Permi[1,2,3,*]

[1]*Department of Biological and Environmental Science, Nanoscience Center, University of Jyvaskyla, P.O. Box 35, FI-40014 Jyvaskyla, Finland*

[2]*Institute of Biotechnology, Helsinki Institute of Life Science, University of Helsinki, Helsinki, Finland*

[3]*Department of Chemistry, Nanoscience Center, University of Jyvaskyla, P.O. Box 35, FI-40014 Jyvaskyla, Finland*

[#]*Present address: Faculty of Medicine and Health Technology, Tampere University, Tampere, Finland*

[*]Corresponding author: Perttu.Permi@jyu.fi

Abstract

Orchestrated action of peptidoglycan (PG) synthetases and hydrolases is vital for bacterial growth and viability. Although the function of several PG synthetases e.g., penicillin binding proteins is well-understood, the function, regulation, and mechanism of action of the majority of PG hydrolases have remained elusive. Lysostaphin-like zinc-dependent metalloendopeptidases specifically hydrolyse the glycyl-glycine peptide bond in the notorious pathogen *Staphylococcus aureus*. In this work, we have employed NMR spectroscopy to study the substrate specificity of the well-established bactericide lysostaphin as well as pre-designated *S. aureus* autolysin LytM. Our results show that the substrate specificities of these highly homologous enzymes are divergent and formerly also inaccurately defined. Yet, we provide substrate-level evidence for the functional role of these enzymes. Indeed, we show that LytM and anti-staphylococcal bactericidin lysostaphin target the D-Ala-Gly cross-linked part of mature peptidoglycan.

Introduction

In the age of antibiotic resistance, multi-resistant bacteria pose a serious threat to global health. This calls for novel strategies to fight the infections[1]. Contemporary means to treat bacterial infections rely on antibiotics. One of the most common mechanisms of action of antibiotics is inhibition of the peptidoglycan (PG) synthesis, a major macromolecular structure in the bacterial cell wall[2,3]. Alarmingly, the Gram-positive bacterium *Staphylococcus aureus* (*S. aureus*) is notorious in developing resistance towards β-lactam based antibiotics e.g., penicillin and their derivatives, which target penicillin binding proteins (PBPs) that are vital for PG synthesis[4]. These methicillin-resistant strains of *S. aureus* (MRSA) can cause life-threatening infections which are very difficult to eradicate[5]. Moreover, although still rarely occurring, outbreaks of infections caused by vancomycin intermediate-level and fully resistant *S. aureus* (VISA/VRSA) are lurking on the horizon[6]. Development of alternative means to treat multi-resistant bacterial infections is therefore needed.

Cell division, cell shape determination, PG remodelling and recycling is administrated and executed by peptidoglycan hydrolases (PGHs), enzymes produced to function as (auto)lysins in the regulation of the cell wall during growth and division[7,8]. On the other hand, PGHs may also function as defensive weapons against other bacterial species as in the case of lysostaphin, an exolysin secreted by *S. simulans* biovar staphylolyticus, which displays bacteriocidic action against competing *S. aureus*[9]. The potential chemotherapeutic role of PGHs is based on the targeted destruction of the protecting PG by hydrolysis, which leads to growing turgor pressure and thus lysis of the bacterial cells[7,9]. Given that PGHs are promising bacteriocins as well as druggable targets for the treatment of multidrug-resistant *S. aureus* infections, profound knowledge of their structure, function as well as substrate specificity is instrumental to harness their full potential as a new breed of antibiotics[10].

S. aureus and other Gram-positive bacteria are protected by a thick PG layer that is composed of repeating β-1,4 linked *N*-acetylmuramic acid (MurNAc) and *N*-acetylglucosamine (GlcNAc) disaccharide units, forming the conserved glycan backbone of murein[7,11] (Fig. 1A-B). Each MurNAc carboxyl group is linked to a stem peptide (L-Ala-D-iso-Gln-L-Lys-D-Ala-D-Ala) and two stem peptides are connected via a cross-bridge structure, the exact composition and length of which depends on the bacterial species in question. In *S. aureus* the cross-bridge is characteristically composed of five glycine residues[7]. Cross-bridging provides an integral structural support for the entire PG wall and allows PG to reach a thickness of over 40 layers (20–80 nm) in Gram-positive bacterial species[7,12].

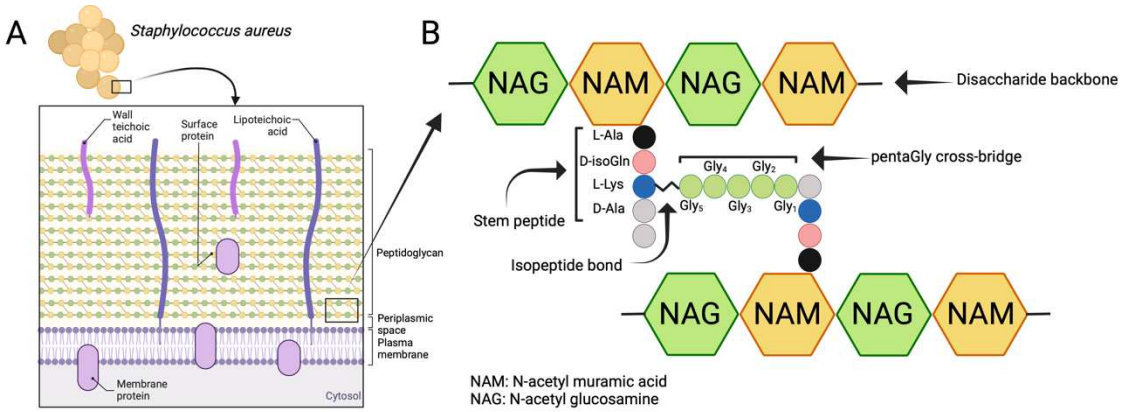

Figure 1. *Structure of the cell wall PG in S. aureus. **(A)** Schematic overview of the cell wall in S. aureus. **(B)** Structure of the peptidoglycan.*

While cell wall composition and biosynthesis of PG are relatively well understood, the perception of PG maintenance and hydrolysis is vague[10]. One prominent PGH family are the lysostaphin-like endopeptidases, which specifically target the cross-bridge peptide bonds of *S. aureus* PG[13,14]. Here we compared LytM and lysostaphin (LSS), which both belong to the zinc-dependent M23 family of metalloendopeptidases and are designated as glycyl–glycine hydrolases. They have been shown to cleave the peptide bonds between glycine residues in the pentaglycine cross-bridge of *S. aureus* PG (Fig. 1B)[9,15–20].

S. simulans LSS, the founding member of the M23 endopeptidase family, is an exolysin possessing bacteriolytic properties towards staphylococci with a pentaglycine cross-bridge structure (e.g. *S. aureus*, *S. carnosus*, *S. cohnii*) (Schindler & Schuhardt, 1964; Schleifer & Fischer, 1982). LytM is a *S. aureus* autolysin with a catalytic M23 domain structurally very similar to that of LSS (Fig. S1). The common fold consists of a characteristic narrow groove formed by a β sheet and four surrounding loops. At one end of the groove resides the catalytic site in which a zinc cation is coordinated by two conserved histidines and an aspartate. The zinc cation, which polarises the peptide bond, and a nucleophilic water molecule activated by two other conserved histidines act in concert to hydrolyse the substrate glycyl-glycine bond[22].

Despite tens of years of effort in studying substrate specificities of LSS-like M23 endopeptidase family members, the exact molecular targets of these enzymes have remained enigmatic, contradictory, and yet imprecise. Interpretation of results is further complicated by diverse conventions used for the numbering of cross-bridge residues. Indeed, the exact cross-bridge bond that LSS targets remains controversial; Browder et *al*. (1965) reported LSS cleavage between glycines 4 and 5 while Sloan et *al*. (1977) observed cleavage of all glycyl-glycine bonds with several substrates of different sizes[23,24]. Recently, using mass spectrometry (MS), Schneewind et *al*. (1995) observed LSS-mediated cleavage between glycines 3 and 4[25]. This observation was supported by a recent NMR spectroscopic study highlighting that hydrolysis by LSS produced fragments in which either two or three glycines are interlinked to the lysine sidechain[26]. On the other hand, Xu et *al*. (1997) reported cleavage at several sites with digested muropeptides: between glycines 1 and 2, 2 and 3 as well as 3 and 4[27]. Additional studies carried out with FRET peptides reported cleavage between glycines 2 and 3 (~60 %) and glycines 3 and 4 (~40 %)[20].

Much less is understood about the functional role of *S. aureus* autolysin LytM. This is partially due to lack of profound knowledge of its substrate specificity. Indeed, based on its high sequence homology with LSS catalytic domain as well as its association with *S. aureus* cell wall maintenance, LytM has implicitly been envisaged to target pGly cross-bridges in the *S. aureus* cell wall. LytM has been shown to hydrolyse pGly into di- and triglycine, and tetraglycine into diglycine[28]. Understanding the substrate specificity is of utmost importance for deciphering the functional role of endogenous LytM in cell division, PG remodelling, antimicrobial resistance, and PG synthesis/hydrolysis in general.

Thus far studies of PG hydrolase specificity have typically utilised end-point kinetics together with LC/MS analysis of digested PG fragments or turbidity reduction assays to determine the site(s) and efficiency of hydrolysis[29,30]. However, these approaches have several pitfalls e.g., they do not provide information on reaction kinetics or atomic resolution of reaction products, which severely limits determination of substrate specificity. In seeking to understand the functional role of these enzymes we have deciphered substrate specificity of LSS and LytM catalytic domains by taking a systematic approach by monitoring hydrolysis of various synthetised PG fragments as well as muropeptides from purified sacculus extracted from *S. aureus* cells using solution-state NMR spectroscopy and utilising turbidity reduction assay on

living *S. aureus* cells. NMR enables following the hydrolysis reaction in real time as well as identification of hydrolysis products.

Here we show that the substrate specificities as well as catalytic efficiencies of M23 family PGHs targeting *S. aureus* PG are different from what has been earlier anticipated. Moreover, our results reveal that quite unexpectedly LytM substrate specificity extends beyond glycyl-glycine endopeptidase activity, which calls for revision of their classification.

Results

Substrate specificities of Lysostaphin M23 enzyme family

Due to inconsistent nomenclature used in the literature to annotate *S. aureus* PG cross-bridge structure and hence substrates used in the enzymatic assays and specificity studies, we conducted a systematic bottom-up approach to delineate the significance of various PG structural elements for the specific activities of LSS and LytM. We prepared a panoply of synthetic peptides faithfully replicating the chemical structure of the recognised *S. aureus* PG fragments (Fig. 2J, Table S1). The common denominator - the scaffold structure - in the PG fragments used in this study, is the pGly cross-bridge as it is uniquely present in *S. aureus* PG (Fig. 1B).

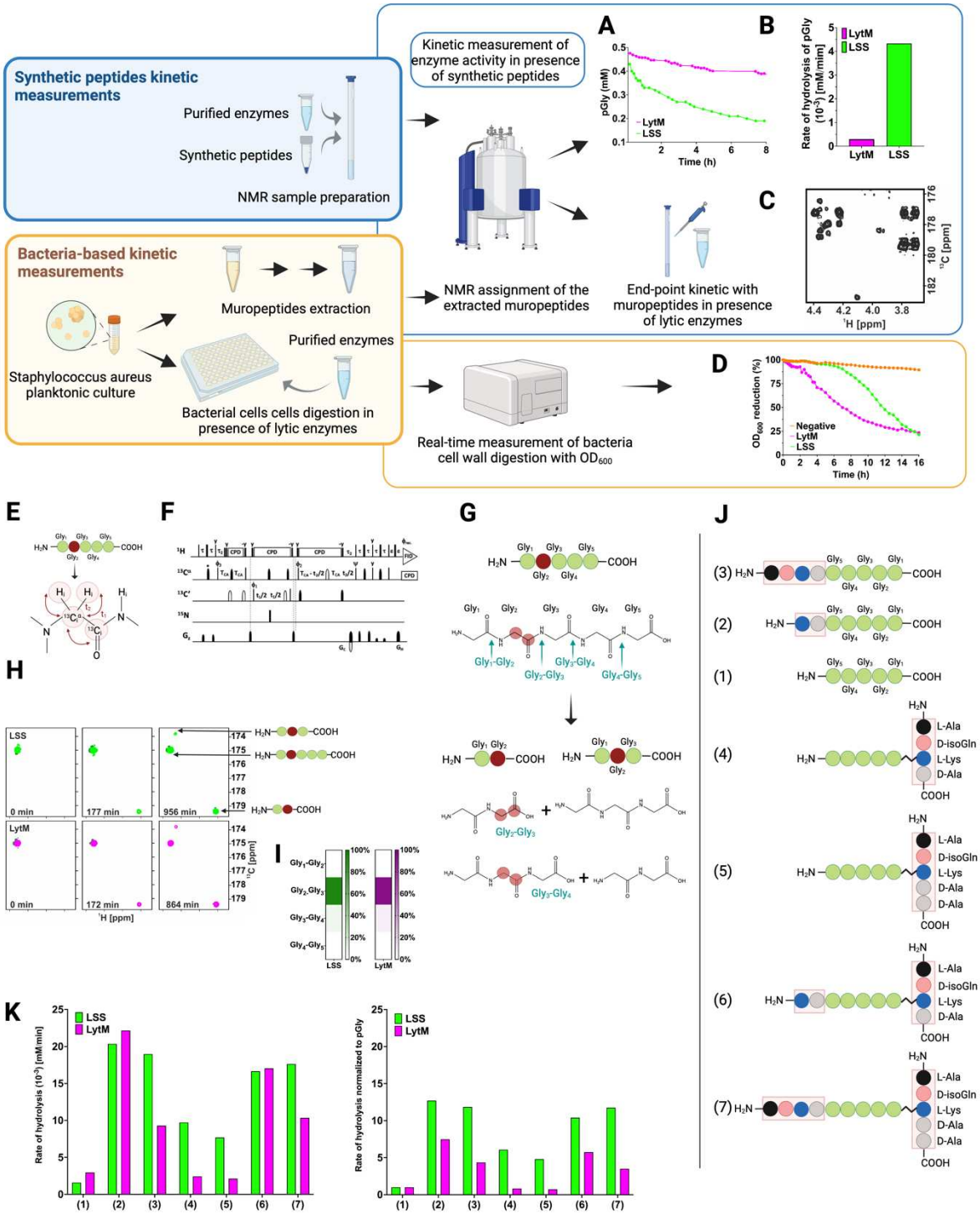

Figure 2. *Workflow to study M23 PGH substrate specificities.* ***Panels in the upper left corner,*** *the two main strategies used in the study. Kinetic measurements carried out with PG fragments (synthetic peptides) were supported by bacteria-based kinetic measurements using S. aureus USA300 cells.* ***Panels in the upper right corner,*** *(**A**) hydrolysis of synthetic pGly (mM) by LSS (green) and LytM (magenta) monitored by ^{1}H NMR spectroscopy over time (h). (**B**) Rate of hydrolysis (mM/min) of pGly derived from A in the first 60 min of the reaction for LSS and LytM. (**C**) ^{13}C-HMBC NMR experiment showing the end-point kinetic of extracted muropeptides from S. aureus USA300 cells. (**D**) Turbidity assay using S. aureus USA 300 cells in the presence of LSS and LytM. The cell lysis is expressed as percentage reduction of the*

bacteria suspension optical density at 600 nm over time (h). ***(E)*** *Pentaglycine hydrolysis by LSS and LytM using Gly_2 ^{13}C -labelled substrate.* ***(F)*** *NMR pulse sequence for the acquisition of glycine Hα-detection optimised 2D HA(CA)CO spectra, showing correlations between $^{1}H\alpha$ and ^{13}CO atoms.* ***(G)*** *With a label the otherwise identical products of the two hydrolysis reactions G_2-G_3, G_3-G_4 can now be differentiated.* ***(H)*** *The appearance of the peaks of the labelled products as a function of time. The labelled glycine has a different CO shift when as G_2 in triglycine or G_2 in diglycine.* ***(I)*** *Heatmap summarising the bond preferences for the enzymes.* ***(J)*** *Depiction of peptides used to study target bond specificity of the enzymes. Hydrolysis of peptides* ***1-7*** *by LSS (green) and LytM (magenta).* ***(K)*** *Initial rates of substrate hydrolysis (mM/min) and* ***(L)*** *the same rates normalised to that of pGly.*

Figure 2 highlights the strategy employed to study substrate specificity and kinetics of LSS and LytM using two different approaches; monitoring hydrolysis of synthetic peptides mimicking PG fragments and muropeptides extracted from *S. aureus* sacculus using solution-state NMR spectroscopy, and monitoring lysis of bacterial cell wall using turbidity reduction assay. In the turbidity reduction assay lytic efficiencies of externally administered LSS and LytM against *S. aureus* USA300 (MRSA) strain were compared (Fig. 2D). These data show that OD_{600} of late stationary cells reduced from 100 % to 25 % in 16 hours for LytM and LSS.

Given that pGly has long been recognised as the common, non-redundant and yet physiological substrate unit for M23 family endopeptidases, we wanted to accurately define substrate specificities, catalytic efficiencies, and the sites of cutting for the catalytic domains of LSS and LytM. To measure the rate of pGly hydrolysis *in vitro*, we added the corresponding enzymes and monitored decaying substrate concentration with respect to reaction time using quantitative ^{1}H NMR spectroscopy (Fig. 2A). Results indicate that LSS hydrolyses pGly 15-fold faster than LytM. *In vitro* hydrolysis rates of pGly (Fig. 2B) and reduction in *S. aureus* USA300 cell turbidities (Fig. 2D) display consistent differences in catalytic efficiencies of LytM and LSS. However, we see that overall, the lytic efficiency of LSS and LytM against USA300 cells is higher than the rate of pGly hydrolysis *in vitro*. This suggests that *S. aureus* cell wall as a macroscopic substrate or cellular milieu differs significantly from the conditions used for the kinetic assay *in vitro* i.e., pGly as a substrate represents a poor model for describing substrate specificity and functional differences of M23 family endopeptidases. As the next step, we therefore determined the scissile bonds in pGly as well as extended substrate specificity studies of these enzymes beyond the pGly cross-bridge.

LSS and LytM preferentially hydrolyse the Gly_2-Gly_3 bond in pentaglycine

We recently showed using a two-dimensional ^{13}C-HMBC NMR experiment that LytU hydrolyses pGly into di- and triglycine[18]. Whether this was the result of hydrolysis of the bond between Gly_2 and Gly_3, and/or between Gly_3 and Gly_4 in pGly remained undefined because the products are the same in both reactions. Selective ^{15}N,^{13}C-labelling (Fig. 2E) breaks the isotopic symmetry of pGly without introducing *per se* any non-physiological tags to the substrate and enables to define the preferred cleavage sites for LSS and LytM in pGly using ^{1}H-^{13}C NMR spectroscopy. As can be appreciated in Figure 2G,H, isotopic labelling of Gly_2 at Cα and CO carbons in pGly allows unambiguous determination of cleavage site, because the characteristic chemical shift of a C-terminal ^{13}CO resonance (179.4 ppm) is markedly different from a non-terminal ^{13}CO chemical shift (173.8 ppm) at physiological pH. Representative two-dimensional $^{1}H\alpha$-^{13}CO correlation maps, collected with the glycine-optimised 2D HA(CA)CO NMR experiment (Fig. 2F) from the selectively Gly_2 ^{13}C-labeled pGly are highlighted in (Fig. 2H). These data clearly show that LytM and LSS are highly specific for the bond between Gly_2

and Gly_3 (> 85-94 %, Fig. 2H). However, residual cleavage activity towards the bond between Gly_3 and Gly_4 is also evident (< 15 %).

The substrate specificity of LytM and LSS is determined by the D-Ala-Gly cross-link between adjacent PG monomers

In the next phase, we sought to understand the role of plausible auxiliary contacts arising from stem peptides flanking the pGly cross-bridge for the substrate specificity of LSS and LytM. To this end, several larger peptides with PG specific extensions around the pGly scaffold were utilised (Fig. 2J). To alleviate complications arising from multiple sites of hydrolysis in pGly, we decided to monitor the rate of substrate hydrolysis rather than the rate of product formation, and to use a similar substrate concentration for all the PG fragments (~0.4 mM) (Fig. S2). These data using substrates **1**-**7** are shown in Figure 2K. Normalisation of the absolute rates with respect to the common scaffold structure, pGly, should reveal on the substrate level the preference of LSS and LytM towards different PG fragments (Fig. 2L).

Clearly, the overall rate of hydrolysis for LytM and LSS increases with peptides that mimic cross-linked PG fragments (Fig. 2K). Indeed, cross-linking L-Lys-D-Ala dipeptide N-terminally to pGly in **2** increased the rate of hydrolysis with respect to **1** by a factor of 12 and 7.3 for LSS and LytM, respectively (Fig. 2L). Further elongation towards the N-terminus (ADiQKDA-GGGGG, **3**) had only incremental contribution to the rate of overall substrate hydrolysis, 16.8 and 3.3 for LSS and LytM, respectively.

Next, we inspected the influence of a stem peptide linked to the C-terminus of pGly on the substrate hydrolysis rate. In PG fragment **4** the stem peptide is linked to the pGly via an isopeptide bond between lysine ε amino group and the C-terminus of pGly. The PG fragment **5** is similar but corresponds to the peptide moiety in a PG monomer (or pentaglycyl-Lipid II) (Fig. 2J). For LSS, the rate of hydrolysis increased by 5- and 4.5-fold for substrates **4** and **5**, respectively. This increase in overall rate of substrate hydrolysis with respect to pGly is roughly two times smaller than for the linear PG fragments **2** and **3** that contain a D-Ala-Gly cross-link. For LytM, the outcome was in stark contrast to the results observed with LSS. Indeed, LytM activity towards PG fragments **4** and **5** dropped to 69 and 49 %, respectively, of that found for **1**.

Next, we studied the significance of capping the pGly moiety from both its termini. PG fragments **6** and **7** both contain an N-terminal D-Ala-Gly cross-linkage in their structure but differ in **6** having a C-terminal tetra- and **7** a pentapeptide stem i.e., the latter has a D-Ala-D-Ala moiety in its structure. For LSS, 10-fold rate enhancements with respect to **1** for substrate hydrolysis were observed, comparable to enhancements with substrates **2** and **3,** indicating that the moiety C-terminal to pGly does not contribute to LSS specificity. Hence, based on these results, it can be deduced that LSS strongly favors substrates that contain a D-Ala-Gly cross-link i.e., **2**, **3**, **6** and **7**. In the case of LytM, rate enhancements of PG fragments **6** and **7** with respect to **1** were 5.5- and 3-fold, respectively, meaning that the branched stem peptide linked to the C-terminal end of pGly has a slight negative effect on LytM specificity. These data indicate that similarly to LSS, LytM is more specific towards substrates **2**, **3**, **6** and **7** i.e., PG fragments that contain a D-Ala-Gly cross-link.

In all, overall rates of substrate hydrolysis using comparative real time kinetics convincingly indicate that LytM as well as LSS prefer mature PG fragments as substrates i.e., PG units that contain a D-Ala-Gly cross-link between two stem peptides. In contrast to the mere end-point kinetics carried out in the past for LytM and LSS, our present results clearly demonstrate the preference of these enzymes for cross-linked PG fragments beyond redundant glycyl-glycine endopeptidase activity. However, the substrate specific real time kinetics assay does not tell

anything about the site(s) of hydrolysis in the substrates. To understand substrate specificity and the physiological role of these PGHs, we inspected the outcome of these reaction assays in more detail.

LSS and LytM display different substrate specificities than earlier anticipated

NMR spectroscopy allows identification of atom connectivities within the substrate and products, enabling determination of site(s) of hydrolysis at atomic resolution. Figure 3A displays the LSS-catalysed hydrolysis of substrate **2**, the simplest of our PG fragments that contains the cross-link between D-Ala and Gly_1 of pGly synthetised by the transpeptidase. Expansion of the region corresponding to the $^1H\alpha$ resonance of D-Ala in the ^1H spectrum of **2** shows that upon hydrolysis of **2**, two products are formed as manifested themselves by increasing concentrations of $KDAG_1$ and $KDAG_1G_2$ (Fig. S3 shows the identification of the product peaks based on ^{13}C-HMBC spectra). Owing to their different chemical structures, the products display separate peaks, resolved at 800 MHz ^1H field, which allows determination of individual reaction rates. Given that the ^1H method we used is quantitative the preferred site of hydrolysis in the PG cross-bridge can be identified based on product concentrations (Fig. 3C-E). These data show that in **2** LSS hydrolyses amide bonds between Gly_1-Gly_2 as well as Gly_2-Gly_3 with a clear preference for the first one.

By coupling real time kinetics data with identification of reaction products, we determined the cutting sites and the reaction rates of the corresponding products for a total of seven PG fragments for LSS and the combined results of their analyses are shown in Figure 3E. The difference in panels C and E is that for the latter we considered only reactions which dominate for the particular PG fragment whereas in the heatmap representation the relative product concentrations at the end of the hydrolysis reaction are shown. These results are consistent with analyses of substrate hydrolysis rates in that they show that LSS clearly favors PG fragments with a D-Ala-Gly cross-link. Pentaglycine or other PG monomers in which Gly_1 is not cross-linked to the stem peptide of the adjacent PG fragment are hydrolysed at slower rate and the cutting site is shifted by one residue downstream compared to the cross-linked ones. In addition, the bond specificity of the hydrolysis reaction increases with D-Ala-Gly cross-linked PG fragments. In this case, LSS favors cutting the amide bond between Gly_1 and Gly_2 and the hydrolysis rate of this bond is several times higher than that of the Gly_2-Gly_3 bond, or those of Gly_2-Gly_3 and Gly_3-Gly_4 bonds in PG monomers devoid of D-Ala-Gly cross-link.

As we reckoned that D-Ala-Gly cross-link is critical for efficient hydrolysis of LSS substrates, we wanted to study how the length of the glycine containing cross-bridge influences substrate hydrolysis (Figs. S4, S5). Substrate **12**, containing four consecutive glycines attached to Lys-D-Ala was hydrolysed between Gly_1 and Gly_2, as well as Gly_2 and Gly_3, exactly like substrate **2**. However, the hydrolysis rate of the Gly_2-Gly_3 bond was 3-fold faster than in the case of **2**. This is probably due to the absence of tetraglycine as a secondary substrate in the reaction i.e., the reaction products resulting from hydrolysis of **12** do not significantly compete with the primary substrate for binding to the LSS catalytic center. Substrate **13** (KDAGGG) was hydrolysed very slowly and **14** (KDAGG) not at all.

We carried out a similar analysis for LytM using the same set of PG fragments (Fig. 4B). The most striking observation is clearly visible in Figure 3B showing hydrolysis of **2** by LytM, which results in formation of products KDA and $KDAG_1$. Indeed, given that LytM is a well-established glycyl-glycine endopeptidase[17,22,28], we were taken by surprise to observe that LytM, in addition to Gly_1-Gly_2 bond hydrolysis, is also able to cleave the D-Ala-Gly_1 amide bond in the *S. aureus* PG cross-bridge whenever the cross-linked D-Ala-Gly structure is available.

We verified that the observed D-alanyl-glycine bond hydrolysis, which has not been reported before this study, is stereospecific and linked to LytM activity. We performed an identical kinetic assay using KLAGGGGG as a negative control. It confirmed that the enzyme is indeed D-enantiomer specific as no cleavage between alanine and glycine was observed (Fig. S6). Further, using a protocol identical to that of LytM we engineered, expressed, and purified the well-established inactive H291A mutant of LytM and tested it with substrate **2**. As expected, LytM H291A showed no activity. The results confirm that in addition to being a glycyl-glycine endopeptidase as reported earlier[17,22,28], LytM belongs to a small family of endopeptidases which cleave the peptide bond between D-Ala and Gly.

In substrates **2** and **6** LytM cleaves between D-Ala-Gly and Gly_1-Gly_2 with approximately equal rates. Using substrate **2** we did not observe a significant concentration-dependent change in the relative reaction rates of D-Ala-Gly and Gly_1-Gly_2 hydrolysis in the [S]/[E] range tested, from 725:1 to 1:2, when [LytM] = 50 μM. For the N-terminally longer substrates **3** and **7**, the balance is shifted in favor of hydrolysis of Gly_1-Gly_2. Regarding substrates lacking the D-Ala-Gly cross-link, LytM seems to disfavor the stem peptide in the C-terminus of pGly and the overall rate of hydrolysis with respect to pGly is diminished more drastically in comparison to LSS.

Analogously to LSS, we compared the rate of hydrolysis of shorter PG fragments with LytM to map the critical length of the glycine-bridge in the substrate needed for the hydrolysis (Figs. S4, S5). Compared to **2**, the rate of hydrolysis did not change drastically when shortening the glycine chain from five glycines to three. However, LytM strongly favored D-Ala-Gly cleavage in **13** (KDAGGG) whereas it preferred Gly_1-Gly_2 cleavage in **12** (KDAGGGG). Unlike LSS, LytM can still hydrolyse **14** (KDAGG). Only the D-alanyl-glycine bond is cleaved, and the reaction is five to ten times slower than hydrolysis of **2**, **12** and **13**. Owing to its D-Ala-Gly cleavage efficiency, we tested whether LytM could also hydrolyse KDAAGGGGG and KDAAA type substrates. However, the former was hydrolysed like pGly that is, no D-Ala-L-Ala cleavage occurred, but KDAAGG and KDAAGGG products were observed instead (not shown). *Enterococci* cell wall PG mimicking peptide KDAAA was not cleaved at all. This data further confirms that LytM is not only a glycyl-glycine endopeptidase but also acts as a D-alanyl-glycine hydrolase.

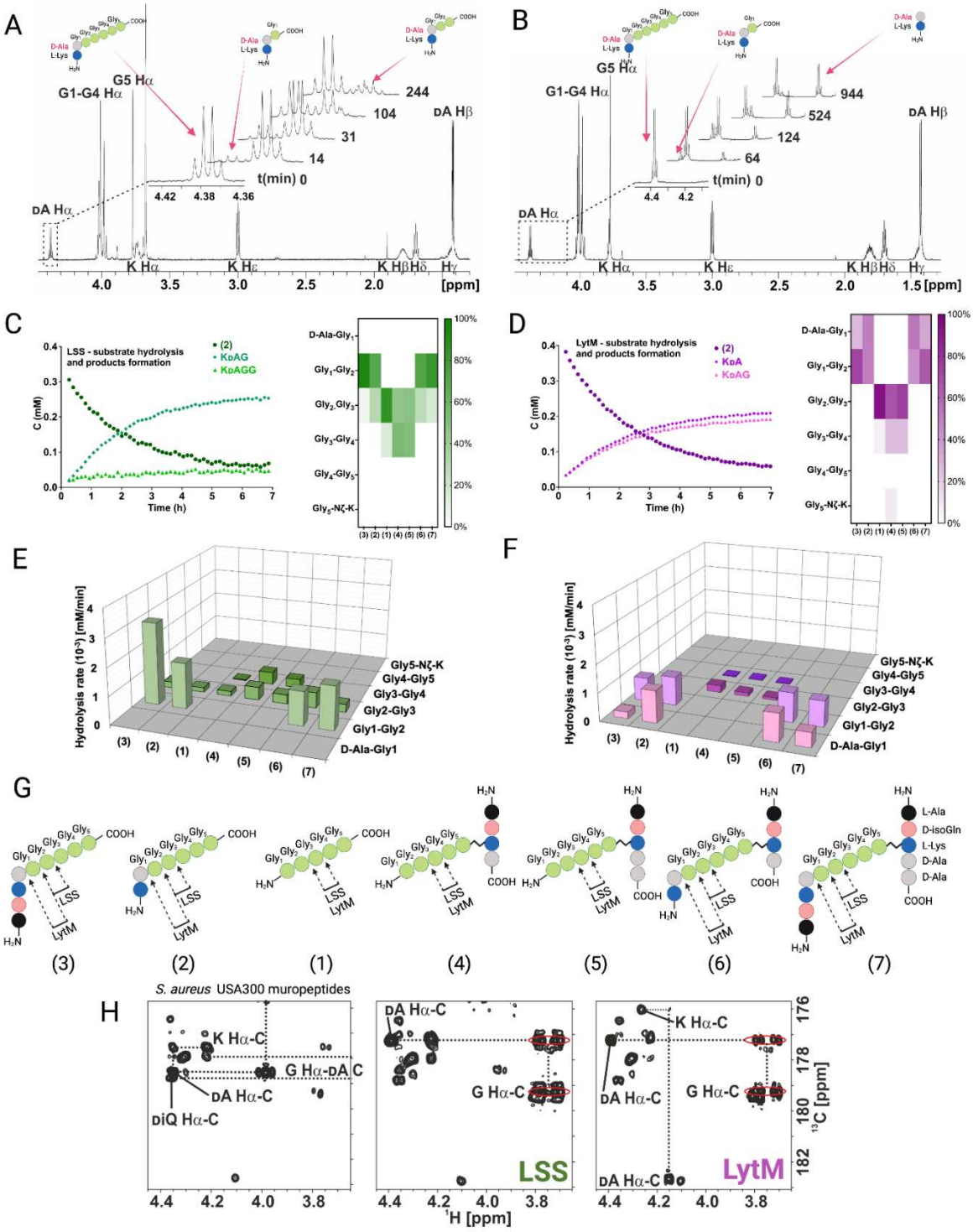

Figure 3. *Hydrolysis of peptides **1-7** by LSS (panels on the left) and LytM (panels on the right). Representative examples of real time NMR monitoring of substrate hydrolysis: Quantitative ^{1}H spectra at selected time points in the hydrolysis reactions of peptide **2** by LSS (**A**) and LytM (**B**). In hydrolysis by LSS peaks of Ala Hα in products KDAG and KDAGG gradually appear as a function of time, whereas in LytM reaction KDA and KDAG are formed. (**C**, **D**) Concentrations in function of reaction time derived from NMR peak integrals for the representative reactions, and on the right, relative product concentrations at reaction end points for the studied PG fragments. **E**, **F**) Rates of formations of products in hydrolyses by LSS and LytM of the studied PG fragments **1-7**. **G**) Bonds cleaved by LSS and LytM in the different PG fragments. **H**)*

Hydrolysis of muropeptides extracted from S. aureus USA300 sacculus by LSS and LytM. On the left, a section of the carbonyl carbon region of the ^{13}C-HMBC spectrum before addition of an enzyme. Middle panel, when LSS is added the bond between alanine and glycine is cleaved and a characteristic peak pattern of an Ala-linked C-terminal glycine Hα appears, encircled in red. On the right, the latter is present also in the spectrum acquired after hydrolysis by LytM. Additionally, the Hα peak of a Lys-linked C-terminal alanine appears.

Hydrolyses of PG fragments mirror scissions in muropeptides extracted from S. aureus USA300 sacculus

To confirm the scissile bond specificity determined for LSS and LytM using synthetic PG fragment mimicking peptides, we extracted and purified muropeptides from *S. aureus* USA300 sacculus using the established protocol[31]. After administering muropeptide samples with LSS and LytM, we observed hydrolysis of the same amide bonds as with corresponding synthetic PG fragments (Fig. 2J). LSS hydrolyses the peptide bond between Gly_1 and Gly_2, recognised as appearance of peak of the C-terminal Gly_1 $^{1}H\alpha–^{13}C'$ resonance correlated with the corresponding $^{1}H\alpha–^{13}C'$ resonance of D-Ala (Fig. 3H). Identical correlations are observed for LytM, indicating that it also hydrolyses the amide bond between Gly_1 and Gly_2 (Fig. 3H). However, additional resonances stemming from the C-terminal D-Ala that is correlated with the neighboring Lys are also observed. This indicates that LytM is cutting both glycyl-glycine and D-alanyl-glycine bonds also in muropeptides extracted from *S. aureus* sacculus.

Differences in susceptibilities of S. aureus mutants towards Lysostaphin and LytM can be explained by their substrate specificities

Composition of the cell wall PG of Staphylococci, including e.g., *S. aureus*, *S. simulans*, *S. epidermidis*, can be modulated by intracellular enzymes. For instance, gene products of *fem* (*f*actor *e*ssential to *m*ethicillin resistance) family members, i.e., femX, femA and femB catalyse nonribosomal insertion of mono- (Gly_5), di-(Gly_4-Gly_3) and di-(Gly_2-Gly_1) glycines into the glycine cross-bridge in *S. aureus* PG, respectively[32]. Reduced susceptibility of *S. aureus* Δ*femB* and Δ*femAB* mutant strains towards LSS has been observed earlier[30,33]. We pondered whether the length of the cross-bridge of *S. aureus* could influence the catalytic efficiency or target bond specificity of LSS and LytM. To this end, we studied hydrolysis of PG fragments **8** and **9** mimicking tri- and monoGly cross-bridge composition of PG in *S. aureus* Δ*femB* and Δ*femAB* mutants, respectively (Fig. 4). Interestingly, LSS hydrolyses **8** with an increased rate as compared to **7**. Furthermore, specificity increases i.e., cutting of glycyl-glycine bond, corresponding to the site "2" in **7** and site "6" in **8**, is not observed. Quite surprisingly, we also observed that LSS is able to hydrolyse substrate **9**, devoid of glycyl-glycine bond. Instead, LSS hydrolyses the Lys Nζ-monoGly C isopeptide bond. The rate of hydrolysis is, however, drastically lower (1.3%) than that of the amide bond between glycines in **7**. This result is excellent agreement with earlier studies on *S. aureus* Δ*femB* and Δ*femAB* mutants and muropeptides extracted from these strains. Indeed, lytic efficiency of LSS against Δ*femB* mutant is not drastically reduced while the minimum inhibitory concentration (MIC) is three orders of magnitude higher for the Δ*femAB* mutant[32]. A dramatic reduction of LSS lytic performance against Δ*femAB* mutants was likewise observed in a turbidity reduction assay[30]. However, residual lytic activity of LSS can be explained by its ability to hydrolyse the Lys Nζ -monoGly isopeptide bond existing in the Δ*femAB* mutant.

Similar results were obtained with LytM except for the scissile bond specificity. Even if the number of glycines in the cross-bridge is reduced from five to three, LytM is still able to hydrolyse both D-Ala-Gly and glycyl-glycine bonds (sites "1" or "5") (Fig. 4). This is in

accordance with results on shortened linear peptides (Fig. S5) as well as with previous turbidity reduction assay data on Δ*femB* mutant[30]. However, if stem peptides are crosslinked with only a single glycine in the cross-bridge (**9**), LytM displays diminished activity by 8-fold in comparison to **7**. Yet somewhat surprisingly, considering the cleavage of D-Ala-Gly bond in substrate **14** (KDAGG, Fig. S5), LytM hydrolysed the Lys Nζ -monoGly C isopeptide bond. This again provides rationale for non-negligible lytic activity observed for LytM on Δ*femAB* mutants although devoid of glycyl-glycine peptide bonds in their cross-bridge[30].

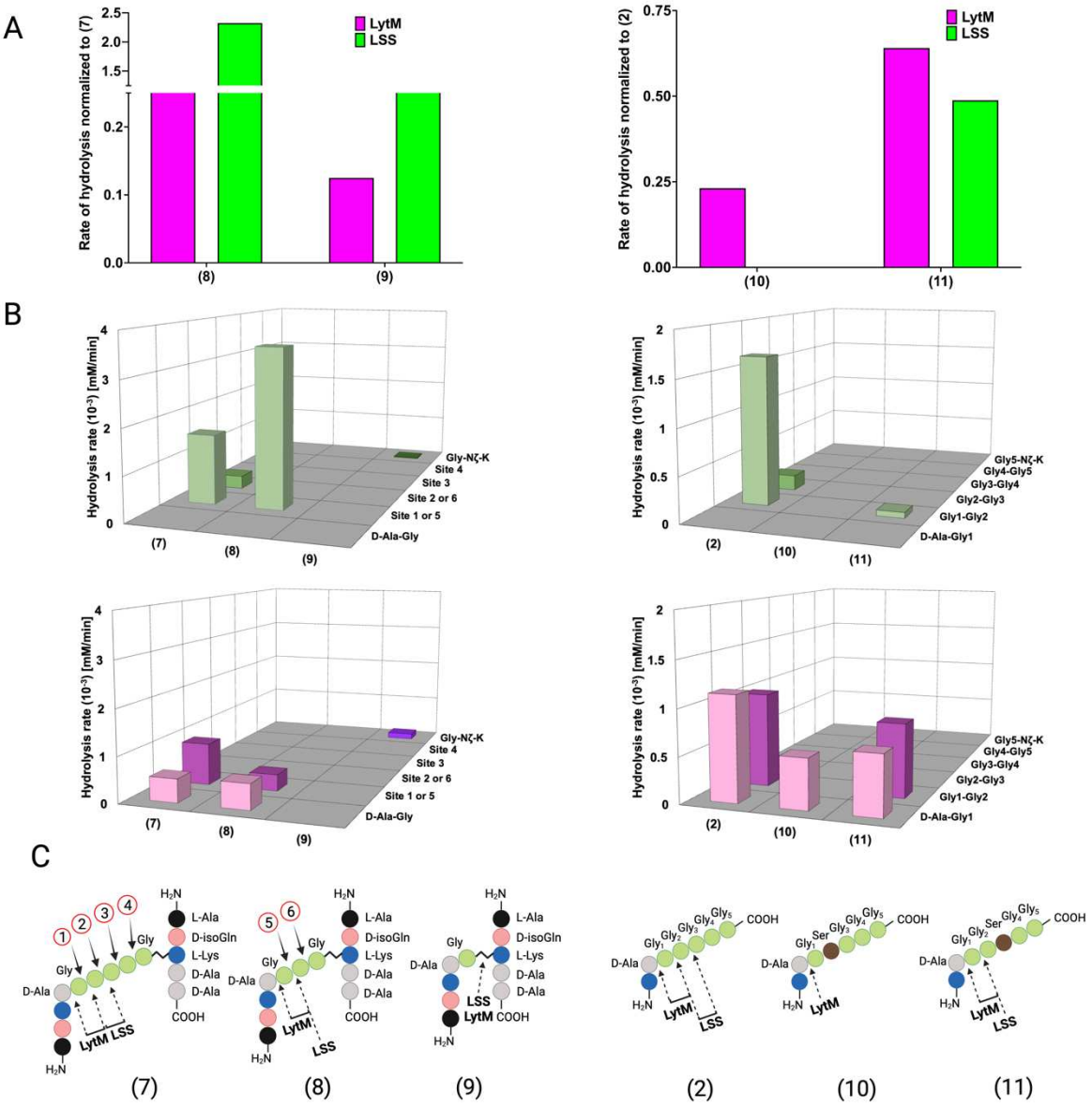

Figure 4. *Hydrolysis of PG fragments with a shorter cross-bridge or with serine in cross-bridge. Rates of substrate hydrolysis (**A**) and formation of product(s) in hydrolysis (**B**) by LSS (green) and LytM (magenta) of fragments **8** and **9** as compared with fragment **7** (panels on the left) and of fragments **10** and **11** as compared with fragment **2** (panels on the right). (**C**) Depictions of structures of used PG fragments.*

Next we tested the activity of LSS and LytM on PG fragments originating from so-called lysostaphin immunity factor (Lif/epr)-containing strains of *S. aureus*, that is the significance of serine substitutions in the PG cross-bridge on substrate hydrolysis[34–36]. Of the two PG

fragments, **10** and **11**, having Gly_2 or Gly_3 replaced by a serine, only **11** was hydrolysed by LSS. LSS cleaved the bond between Gly_1 and Gly_2 in **11** although with a rate 30-fold slower than that for substrate **2**. The results with LSS correlate well with earlier observations that show only fractional lytic activity of LSS towards *Staphylococcal* strains with serine in the cross-bridge[30]. LytM was able to hydrolyse both PG fragments. **11** was cleaved similarly to the PG fragment **2**, whereas LytM specifically cleaved the D-Ala-Gly amide bond in **10** as it contains serine in the second position. The rates of substrate hydrolysis were not drastically lower i.e., by a factor of 4.3 (**10**) and 1.5 (**11**) in comparison to **2**. These data provide rationale to the observed differences in lytic efficiencies of LSS and LytM on *S. aureus* cells having serine substitutions in the cross-bridge[30]. Hence, given that LytM exhibits significant catalytic activity towards D-Ala-Gly cleavage, it is less susceptible to serine substitutions in the cell wall PG. LytU hydrolysed only the amide bond between Gly_3-Gly_4 in **10** and no activity was detected with **11** as serine substitution for Gly_3 results in non-scissile bonds Gly_2-Ser_3 and Ser_3-Gly_4 in **11**. The effect of serine in a fragment containing an isopeptide bond was not tested in this study.

Structural level perspective on deviating substrate specificities for LSS and LytM

We combined the detailed substrate-level information in terms of real time reaction kinetics and scissile bond specificities together with the existing structural models available for LSS and LytM to glean structural-level understanding of enzyme specificities. Based on these data and using the nomenclature formulated by Schechter and Berger[37], we delineated substrate specificities for LSS and LytM (Fig. 5). It is clear that LSS is a glycyl-glycine endopeptidase as P1 and P1' positions are invariably occupied by Gly residues. However, the rate of hydrolysis increases when D-Ala occupies the P2 position, that is when LSS recognises a D-Ala-Gly cross-link in the cell wall. LytM is flexible regarding the P1 site, it can be accommodated either by D-Ala or Gly, whereas the P1' position is invariably occupied by Gly.

Why does LytM hydrolyse a D-Ala-Gly bond but LSS does not? To address this intriguing question, we utilised the existing structure of LytM in complex with the transition state analog tetraglycine-phosphinate [22] and used molecular modelling approach to dock PG fragment **2** into the active sites of LSS and LytM. As has been proposed earlier, the Zn^{2+} at the active site polarises the scissile bond by coordinating the carbonyl oxygen of a residue in the P1 position. For LytM this is either D-Ala or Gly, and for LSS it is Gly (Fig. 5). D-Ala in the P1/S1 position in the LSS active site results in a steric clash with loop 1, most notably its residues L272-I274, thus preventing hydrolysis of a D-alanyl-glycine peptide bond. In LytM the corresponding loop is shorter allowing accommodation of D-Ala in the P1/S1 position and hence cleavage of D-alanyl-glycine cross-bridge or alternatively, if the substrate has a Gly in the P1 position, the peptide bond between Gly_1 and Gly_2.

The same loop 1 gates the LSS active site and establishes the structural basis for Lif function. Serine in the P2' position severely hinders accommodation of the substrate to the LSS active site, which results in a drastic drop in the rate of hydrolysis (Fig. 5). In LytM the three residues shorter loop renders the active site more voluminous, which permits the short polar sidechain of Ser to fit in to the P2' or P3' positions. Consequently, substrates **10** (KDAGSGGG) and **11** (KDAGGSGG) can still be hydrolysed with relatively high efficiency (ca. 50%) in comparison to PG fragment **2** which contains a pGly bridge. Interestingly, as the P1' position only allows Gly, **10** cannot be hydrolysed between Gly_1 and Ser_2. However, LytM is able to hydrolyse the D-alanyl-glycine bond due to the positioning of the Ser into the P2' position. LSS cannot hydrolyse **10** as it would require the disallowed P1' position to accommodate Ser or alternatively P1 to be occupied by D-Ala, both of which are prevented by the extended loop 1 structure in LSS.

Interestingly, when the D-Ala-Gly cross-link is missing e.g., in pGly or PG fragments **4** and **5**, the latter mimicking a non-cross-linked PG monomer, the cleavage site is shifted within the glycine cross-bridge that is, cutting occurs between Gly_2 and Gly_3 since in minimum a substrate with four residues occupying P2, P1, P1' and P2' sites is required for both LSS and LytM. Owing to this limitation in substrate size and distinct difference in the substrate specificity of LSS and LytM, we observe that while both enzymes can hydrolyse tetraglycine, only LytM can cleave **14** (KDAGG) since it accepts D-Ala in the P1 position. We observed significant reduction in rate of hydrolysis for both LSS and LytM when the substrate is too short i.e., it cannot fill the P3'/S3' position. This is probably due to the stabilising hydrogen bonds that are formed between the longer glycine chain and a key asparagine residue in loop 4, Asn372 and Asn303 for LSS and LytM, respectively (Fig. 5B, F).

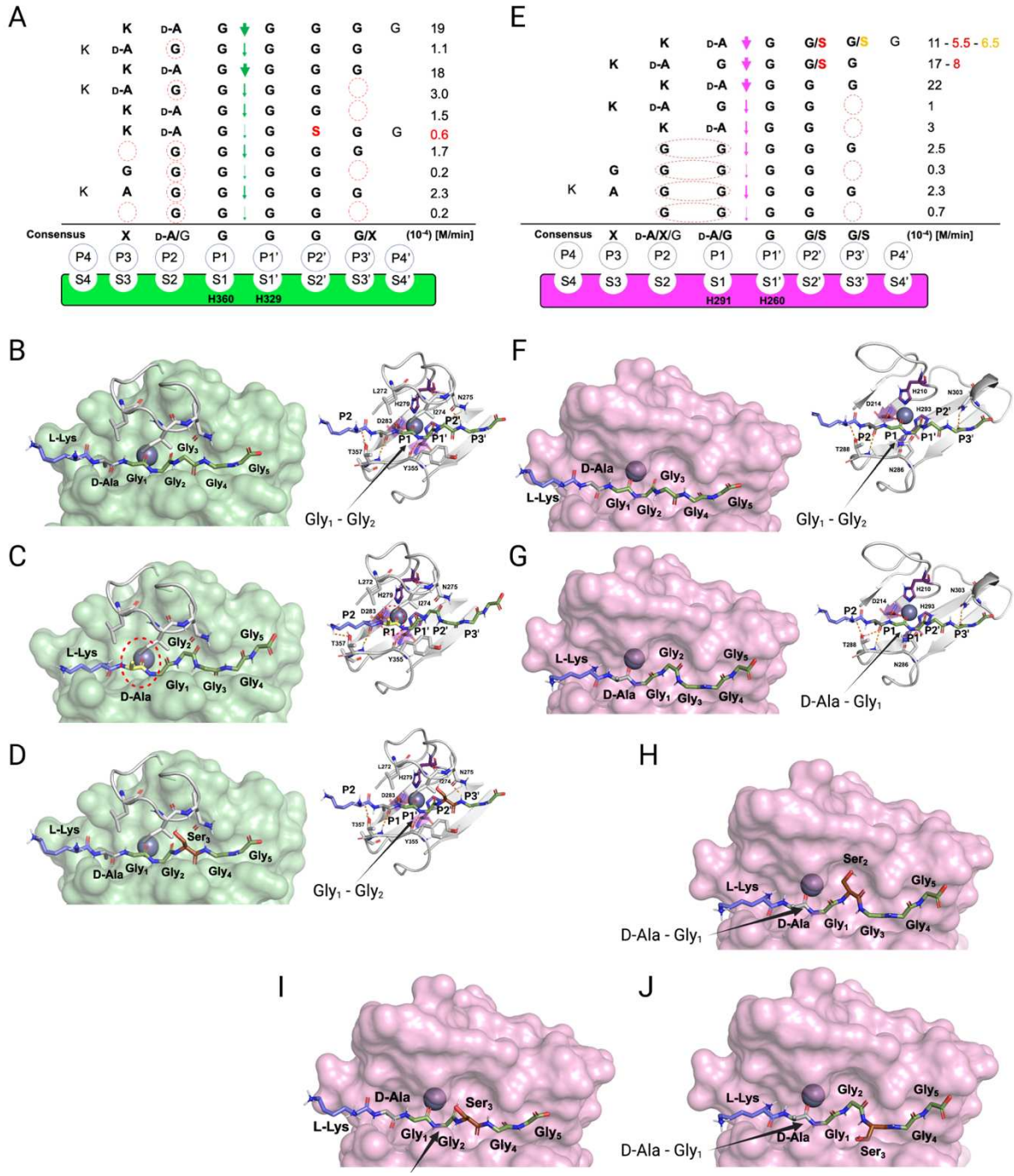

Figure 5. Substrate specificity of LSS and LytM*. Schechter and Berger nomenclature is employed to describe the differences in substrate specificity between LSS (panel **A**) and LytM (panel **E**). Scissile bond in the substrate is between the P1 and P1' positions, indicated by green (LSS) and purple arrows (LytM), and hence residues towards the N-terminus from the scissile bond are P1-P4, whereas those towards the C-terminus are designated as P1'-P4'. PG fragments devoid of stem peptide linked to the C-terminal glycine are shown aligned with respect to their cleavage sites together with the rate of hydrolysis of the particular scissile bond. Consensus sequence displays preferable amino acid(s) that are accepted in the specific position (...P2, P1, P1', P2'...) with respect to the cleavage site. Red circles/ovals indicate missing or less than optimal amino acid accommodation in the particular P site, which translates into reduced catalytic efficiency. Serine substitutions in the glycine bridge and associated rates of hydrolysis are indicated by red and orange colors. Panels **B-D** show the docking results for fragments **2** and **11** into the catalytic site of LSS and panels F-J show the docking results for fragments **2**, **10**, and **11** into the catalytic site of LytM. LSS and LytM are capable of cleaving the Gly_1-Gly_2 bond in **2** (Panels **B, F**). LytM is also able to cleave the D-Ala-Gly_1 bond (Panel **G**), however, in LSS this would result in a steric clash between the D-Ala side chain and the residues in loop 1 (Panel **C**).*

Discussion

To gain novel insight into lysostaphin enzyme family specificities, we employed NMR spectroscopy to determine the substrate specificities using real-time kinetics at atomic resolution on substrates mimicking PG fragments. In addition, we verified the sites of hydrolysis on muropeptides purified from *S. aureus* USA300 sacculus and confirmed lytic efficiencies of LSS and LytM with turbidity reduction assays on bacterial *S. aureus* USA300 cells.

Previous research on substrate specificity is largely based on testing several bacterial strains with varying PG composition[17,30] either with lysis assays or purified PG. Thus, determination of the site of hydrolysis often relies on applying abductive reasoning to either include or exclude different PG structures according to the assay results. Because this type of experimental set up often does not reveal the direct cleavage site, nor if there are several cleavage sites it should be supplemented with methods allowing direct observation – such as NMR. Yet, the end-point kinetics type of enzymatic assays e.g., administering chromatographically purified muropeptides with a lytic catalyst and quenching the reaction after overnight incubation, followed by mass spectrometric analysis of reaction products, do not necessarily reflect substrate specificity accurately because they only detect reaction products at the end and do not consider plausible secondary reactions.

Our method is superior to the previous approaches because real-time kinetics data combined with a precise determination of the bond cut-off point reveal the true substrate specificity of LSS. Our data also explain the inconsistencies between results of previous studies, that is, our extensive set of PG fragments allowed a more comprehensive interpretation than previous studies with fewer substrates[15,20,23–27,30,32,38,39]. LSS recognises the D-Ala-Gly cross-link. In such a substrate, D-Ala occupies the P2 position, which increases the rate of hydrolysis by 10-fold in comparison to substrates which position glycine into P2 (Fig. 5). As mature PG in *S. aureus* cell wall is highly (D-Ala-Gly) cross-linked, our results are in excellent agreement with the observed efficiency of LSS towards *S. aureus* cells in numerous studies in the literature [30,40]. We also showed that LSS can hydrolyse cell wall in the *S. aureus* Δ*femB* mutants[33], having three glycines in the cross-bridge, as they contain cross-linked D-Ala-Gly which occupy the P2-P1 positions and two glycines accommodated in the P1'-P2' positions (Fig. 5A). However, our

data also demonstrate that LSS is capable of efficiently hydrolysing glycyl-glycine bonds in PG fragments with different levels of cross-linking, including also non-cross-linked PG monomers. In such a case, Gly_1 and Gly_2 house the P2 and P1 positions and the scissile bond is shifted from the preferable Gly_1-Gly_2 bond one residue forward to the Gly_2-Gly_3 amide bond. This confirms the findings made by Maya-Martinez and colleagues with non-cross-linked PG fragments i.e., LSS leaves two or three glycines connected to Lys sidechain[26].

Hence, our results provide rationale to the previous observations which show discrepancy regarding the LSS site of hydrolysis. To summarise, LSS prefers cutting between Gly_1 and Gly_2, whenever Gly_1 is cross-linked to D-Ala of neighboring stem, whereas it hydrolyses the amide bond between Gly_2 and Gly_3 in non-cross-linked (devoid of D-Ala-Gly bond) PG fragments.

LytM was originally categorised as a glycyl–glycine endopeptidase based on lytic experiments performed using purified cell walls, which showed that it is active against S. *aureus* and *S. carnosus* but not against *Micrococcus luteus*[17]. *M. luteus* PG has the following structure: Ala-(D-γGlu-Gly)-Lys[D-Ala-Lys-D-Glu(-Gly)-Ala-D-Ala-Lys-D-γGlu(-Gly)-Ala]-D-Ala and thus contains neither Gly-Gly nor D-Ala-Gly bonds[14]. As was suggested by Ramadurai et *al*. (1999)[17] *M. luteus* lacked the bond necessary for LytM cleavage, and here we have identified that bond to be D-Ala-Gly in addition to the known specificity towards glycyl–glycine bonds.

The only other recognised D-Ala–Gly hydrolase in *S. aureus* is LytN. Contrary to LytM, it contains a catalytic CHAP domain, which cleaves both D-Ala-Gly and MurNAc-L-Ala bonds, in other words is a D-alanyl-glycine endopeptidase as well as an N-acetylmuramoyl-L-alanine amidase domain[29]. D-Ala-Gly cleavage activity has also been found from a CHAP domain of a *S. aureus* Phage ϕ11 murein hydrolase. In this hydrolase amidase activity is contained in another domain of the modular protein [39]. Recently also *Enterococcus faecalis* EnpA, which belongs to the M23 metalloendopeptidase family, has been shown to cleave D-Ala-Ala bond in *E. faecalis*. D-Ala-Gly cleaving activity was also reported, although without quantitative information regarding catalytic efficiency. Given that the P1 site in EnpA can accommodate D-Ala, it exhibits substrate specificity similar to that of LytM, which allows occupation of the P1 position by D-Ala (and Gly). In this way, LytM and EnpA deviate from LSS which requires invariably glycine in the P1 position. On the other hand, similar to LSS, LytM allows only glycine at the P1' site, whereas EnpA is more promiscuous and can accommodate Gly, L-Ala and L-Ser in this position[30,38].

The pivotal findings in this paper are the discovery of the D-Ala-Gly hydrolysis activity of LytM, previously designated solely as a glycyl-glycine endopeptidase. Yet, we show for the first time that the substrate specificity of LSS is defined by the D-Ala-Gly cross-link, which increases catalytic efficiency 10-fold with respect to pentaglycine.

Methods and materials

Reagents

Peptides were synthetised by CASLO as Trifluoroacetic acid (TFA) salts. *Escherichia coli* BL21 (DE3)pLysS cells were obtained from Novagen (Novagen). *Staphylococcus aureus* USA300 and Newman D2C RN4220 cells were purchased from American Type Culture Collection (ATCC). The *S. aureus* Newman conditional overexpressing LytU RH7781 mutant was previously described[18].

Protein expression and purification

The catalytic domain of LSS (LSS_{cat} residues 248-384) was produced as a His-tagged GB1-fusion protein. LSS_{cat}GB1 was cloned in pET15b vector (Novagen) and heat-shock transformed into *E. coli* BL21(DE3) pLysS (Novagen). The cells were grown at 37 ºC with 250 rpm orbital shaking in Luria-Bertani broth supplemented with 100 µg/ml ampicillin until the OD_{600} reached 0.55-0.6. Then the temperature was lowered to 20 °C and protein expression was induced by adding 0.4 mM isopropyl β-D-1-thiogalactopyranoside (IPTG). The overexpression of the proteins occurred at 20 ºC for 20 hours. The cells were harvested by centrifugation at 6000 g for 20 min at 20 ºC followed by cell resuspension in 1x PBS buffer and stored in -80 °C until purification. Complete lysis of the cells was achieved using Emulsiflex-C3 homogeniser (Avestin) and lysates were cleared by centrifugation at 35,000g for 30 min at 4 °C. The 6x-His-tagged proteins were captured using Ni-NTA Superflow (QIAGEN) and the His-tag was cleaved at 4 ºC for 16-18 hours by human thrombin (Biopharm laboratories). HiLoad 26/60 Superdex 75 pg column (GE Healthcare) was utilised in the size exclusion chromatography of the desired fragments in 20 mM Sodium-phosphate buffer pH 6.5, 50 mM NaCl using an ÄKTA pure system (GE Healthcare).

LytM catalytic subunits ($LytM_{cat}$ residues 185-316) were cloned into pGEX-2T vector and heat-shock transformed into *E. coli* BL21(DE3)pLysS (Novagen). The GST fusion $LytM_{cat}$ protein was produced the same way as LSS_{cat}GB1. The GST fusion proteins were purified with Protino Glutathione Agarose 4B (Macherey-Nagel) and GST was cleaved by human thrombin (Biopharm laboratories) at 4 ºC for 16 h. The protein was further purified by size exclusion chromatography (SEC) with a HiLoad 26/60 Superdex 75 pg column (GE Healthcare) in SEC buffer (20 mM Sodium-phosphate buffer pH 6.5, 50 mM NaCl) using an ÄKTA pure chromatography system (GE Healthcare). Eluted fractions were concentrated using Amicon® Ultra to 1 mM final concentration.

The inactive mutant of LytMcat (LytMcat_H291A) was generated using QuikChange II Site-Directed Mutagenesis kit (Agilent Technologies) and the mutation was verified by sequencing. The recombinant proteins were produced and purified same as the wildtype.

The ^{15}N-labelled $LytM_{cat}$, and $LytM_{cat}$_H291A were expressed in *E. coli* BL21(DE3)pLysS cells in standard M9 minimal medium using 1 g/l ^{15}N NH_4Cl (Cambridge Isotope Laboratories) as a sole nitrogen source. The proteins were purified in 50 mM NaH_2PO_4, pH 6.5, 50 mM NaCl using the same protocol as described above for the unlabelled proteins.

Muropeptide extraction

Muropeptides were extracted as before described with modifications [31]. 2 mL of overnight bacteria culture were centrifuged at 10,000 rpm in table microcentrifuge, supernatant was discarded, and bacteria were resuspended in 4 mL of 100 mM Tris HCl pH 6.8, 0.25% Sodium dodecyl sulfate (SDS) to reach OD_{600} equal to 10. After boiling SDS was removed with extensive washes. Cells were then solubilised with 1 mL of dH_2O and incubated for 30 min at room temperature in sonifier waterbath. 500 µL of 15 µg/mL DNase in 0.1 M Tris HCl pH 6.8 solution was added and sample was incubated 1 hour at 37 °C, 150 rpm. 500 µL of 4 mg/mL Pronase (Sigma) were added and sample was incubated overnight at 37 °C, 150 rpm. After enzymes inactivation, the pellet was resuspended with 500 µL of 1 M HCl solution and incubated for 4 hours at 37 °C, 150 rpm to release the teichoic acid. The sample was then washed with dH_2O until pH was between 5 and 6. Finally, the pellet was resuspended with 12.5 mM sodium dihydrogen-phosphate, pH 5.5 or 20 mM sodium phosphate buffer pH 6.5 and adjusted to OD_{578} equal to 3; Mutanolysin (Sigma) solution 5000 U/mL was added and incubated for 16 hours at 37 °C, 150 rpm. After mutanolysin inactivation, sample was

centrifuged at 10,000 rpm in table microcentrifuge for 10 min, pellet was discarded and muropeptides were in the supernatant. Muropeptides were dried using Savant SC110A SpeedVac (Thermo Fisher Scientific), resuspended with D_2O and pH was adjusted to 7.5 using deuterated sodium hydroxide. NMR sample was prepared by diluting the muropeptides stock solution in 50 mM dTRIS 7.5, and 0.1 mM DSS as reference compound.

Sample preparation for NMR kinetics

The synthetic peptides were purchased from CASLO. The peptides were resuspended in D_2O at the concentration of 20-40 mM, except for Gly_2 position ^{13}C-labeled pGly which was 6.5 mM. For all peptides the pH was adjusted to 7.5 using deuterated sodium hydroxide. Peptides were diluted to a desired concentration in presence of 50 mM deuterated TRIS pH 7.5. For each sample, prepared to 3 mm OD round bottom NMR tube, 0.1 mM Sodium trimethylsilylpropanesulfonate (DSS, Chenomx Internal standard, 5 mM 99,9 % D, lot PS20190624) was added as a reference compound. Reactions were initiated by adding the enzyme to a final concentration of 2 µM or 50 µM.

NMR-based kinetics and resonance assignment of synthetic PG fragments and muropeptides from *S. aureus* sacculus

All NMR experiments were carried out at 25 °C, and at the field strength of 800 MHz of ^1H frequency on a Bruker Avance III HD NMR spectrometer, equipped with cryogenically cooled ^1H, ^{13}C, ^{15}N triple-resonance TCI probehead. NMR data collection for kinetics measurements employed a standard ^1H pulse program (zgpr) having a selective radiofrequency field for residual HDO signal presaturation during the recycle delay. To ensure quantitative detection of substrate and product concentrations, a 20 second long recycle delay was used between the transients used for the signal averaging. 0.1 mM DSS was used as a reference compound both for the peak integration, chemical shift referencing as well as lineshape optimisation. For each time point, experiment was accumulated with 24 transients, yielding an experimental time of 8 minutes per time point.

First, a reference ^1H spectrum was acquired. The sample was then removed from the magnet, and the enzyme was added. The time of enzyme addition was recorded as t=0. After the enzyme addition the sample was placed back into the magnet, and the shim was manually readjusted before the start of acquisition of consecutive ^1H spectra to follow the hydrolysis. This preparatory work resulted in a delay of about 5-10 minutes between enzyme addition (t=0) and the end of the acquisition of the first spectrum. This delay was accounted for in the data analysis for each experiment.

For the resonance assignment of NMR $^1H\alpha$, $^{13}C\alpha$ and ^{13}CO chemical shifts in selectively ^{13}C-labeled Gly_2 position in pentaglycine (**1**), a glycine Hα-detection optimised HCACO -type NMR experiment was devised (Fig. S7). The spectrum was collected as a 2D H(CA)CO ^1H-^{13}C correlation experiment to establish connectivities between $^1H\alpha$ and ^{13}C' resonances in Gly_2. The experiment was measured using 2 transients per FID and the overall experimental time was 200 seconds per time point.

Assignment of chemical shift resonances in different synthetic PG substrates and products as well as muropeptides from *S. aureus* USA300 sacculus was based on the measurement of ^1H as well as 2D ^1H-^{13}C HSQC, ^1H-^{13}C HMBC, and ^1H-^{13}C' selective HMBC spectra. Typically, ^1H-^{13}C HMBC experiments were measured overnight and at the end of the reaction to warrant the highest sensitivity for product chemical shift assignment.

Data analysis of NMR kinetics

To obtain substrate and product concentrations at each time point, NMR resonances were integrated together with reference compound using Topspin 3.6.5 software package (Bruker). Rates of reactions were calculated using linear regression of the first 40-60 min of the reaction. Goodness of fitting was evaluated by using the R^2 value. All the data fitting had $R^2 >= 0.9$. Rates of the reaction *versus* substrate concentrations were plotted and Michaelis-Menten fitting was performed using GraphPad Prism software version 9.5.1 (GraphPad Software Inc.).

***Staphylococcus aureus* cell growth conditions**

Staphylococcus aureus USA 300 cells were grown overnight in Tryptic Soy Broth (TSB) and Newman RN4220 and RH7781 were grown in Lysogeny Broth (LB) at 37 °C, 200 rpm by inoculating one single colony in 3 mL of medium. Bacteria were then diluted 1:100 in prewarmed TSB and grown until desired OD_{600}.

Turbidity reduction assay

Turbidity assay was performed as previously described with some modifications [18]. *S. aureus* USA 300 bacterial cells were incubated at 37 °C, 200 rpm until OD_{600} between 6 to 8 corresponding to late stationary phase. Bacteria were then washed twice using 20 mM Tris HCl pH 7.5, 50 mM NaCl, and resuspended at OD_{600} equal to 5. Bacteria were plated in round-bottom 96-well plate (Thermo Fisher Scientific), and the reaction was started by adding the enzymes at final concentration of 50 µg/mL. The assay was carried out in final volume of 100 µL. Bacteria without any enzyme was used as control sample. Reduction of turbidly of bacteria suspension was followed using BioTek Epoch2 Microplate Spectrophotometer (Agilent Technologies), at 25 °C for 16 hours with continuous shaking at 500 cpm. Data were expressed as normalised reduction of the turbidity over the time. Each reaction was carried out in quadruplicate.

Docking

Substrate **2** for docking was built with Maestro molecular modeling software (Schrödinger, 2021) available in Schrödinger (LLC, New York, NY) and Ligprep ligand preparation tool was used to refine the structure with force field OPLS4. The crystal structures of LytM (PDB code: 4ZYB, (23)) and lysostaphin (PDB code: 4QPB, [39]) were retrieved from the Protein Data Bank. The protein structures were first prepared with the Protein preparation wizard available in the Schrödinger suite. Protein preparation wizard was used to add missing hydrogen atoms, delete water molecules, and assign correct bond orders with force field OPLS4. Glide [42–44] was used for docking. The receptor grid was generated with Glide and the Standard Precision (SP) Peptide mode was used for docking. It was noticed that the scoring function favors the strong interaction between the carboxylic acid of the substrate C-terminus and zinc ion, and thus the C-terminus was capped with an N-methylacetamide (NMA) residue. The serine containing peptides were modeled in the binding site by mutating the appropriate residues with Pymol [45].

Acknowledgements

We thank Dr. Maarit Hellman for expert technical assistance. This work was supported by the grants from the Academy of Finland and Jane and Aatos Erkko foundation. Part of the figures were made using BioRender.com.

Conflict of Interests

The authors declare that they have no conflict of interest.

References

1. Shrivastava, S. R., Shrivastava, P. S. & Ramasamy, J. World health organization releases global priority list of antibiotic-resistant bacteria to guide research, discovery, and development of new antibiotics. *JMS - Journal of Medical Society* **32**, 76–77 (2018).
2. Džidić, S., Šušković, J. & Kos, B. Antibiotic resistance mechanisms in bacteria: Biochemical and genetic aspects. *Food Technol Biotechnol* **46**, 11–21 (2008).
3. Kapoor, G., Saigal, S. & Elongavan, A. Action and resistance mechanisms of antibiotics: A guide for clinicians. *J Anaesthesiol Clin Pharmacol* **33**, 300 (2017).
4. Sauvage, E., Kerff, F., Terrak, M., Ayala, J. A. & Charlier, P. The penicillin-binding proteins: structure and role in peptidoglycan biosynthesis. *FEMS Microbiol Rev* **32**, 234–258 (2008).
5. Lee, A. S. *et al.* Methicillin-resistant Staphylococcus aureus. *Nat Rev Dis Primers* **4**, 18033 (2018).
6. Shariati, A. *et al.* Global prevalence and distribution of vancomycin resistant, vancomycin intermediate and heterogeneously vancomycin intermediate Staphylococcus aureus clinical isolates: a systematic review and meta-analysis. *Sci Rep* **10**, 12689 (2020).
7. Ghuysen, J. M. Use of bacteriolytic enzymes in determination of wall structure and their role in cell metabolism. *Bacteriol Rev* **32**, 425–464 (1968).
8. Wang, M., Buist, G. & van Dijl, J. M. Staphylococcus aureus cell wall maintenance – the multifaceted roles of peptidoglycan hydrolases in bacterial growth, fitness, and virulence. *FEMS Microbiol Rev* **46**, fuac025 (2022).
9. Schindler, C. A. & Schuhardt, V. T. Lysostaphin: a new bacteriolytic agent for the Staphylococcus. *Proceedings of the National Academy of Sciences* **51**, 414–421 (1964).
10. Szweda, P. *et al.* Peptidoglycan hydrolases-potential weapons against Staphylococcus aureus. *Applied Microbiology and Biotechnology* vol. 96 1157–1174 (2012).
11. Schleifer, K. H. & Kandler, O. Peptidoglycan types of bacterial cell walls and their taxonomic implications. *Bacteriol Rev* **36**, 407–477 (1972).
12. Kim, S. J., Chang, J. & Singh, M. Peptidoglycan architecture of Gram-positive bacteria by solid-state NMR. *Biochimica et Biophysica Acta (BBA) - Biomembranes* **1848**, 350–362 (2015).
13. Ghuysen, J.-M., Tipper, D. J. & Strominger, J. L. Enzymes that degrade bacterial cell walls. in *Methods in Enzymology* 685–699 (1966).
14. Vollmer, W., Joris, B., Charlier, P. & Foster, S. Bacterial peptidoglycan (murein) hydrolases. *FEMS Microbiol Rev* **32**, 259–286 (2008).
15. Bardelang, P. *et al.* Design of a polypeptide FRET substrate that facilitates study of the antimicrobial protease lysostaphin. *Biochemical Journal* **418**, 615–624 (2009).
16. Odintsov, S. G., Sabala, I., Marcyjaniak, M. & Bochtler, M. Latent LytM at 1.3 Å Resolution. *J Mol Biol* **335**, 775–785 (2004).
17. Ramadurai, L., Lockwood, K. J., Lockwood, J., Nadakavukaren, M. J. & Jayaswal, R. K. Characterization of a chromosomally encoded glycylglycine endopeptidase of Staphylococcus aureus. *Microbiology (N Y)* **145**, 801–808 (1999).
18. Raulinaitis, V. *et al.* Identification and structural characterization of LytU, a unique peptidoglycan endopeptidase from the lysostaphin family. *Sci. Rep.* **7**, 6020 (2017).

19. Tossavainen, H. *et al.* Structural and functional insights into lysostaphin-substrate interaction. *Front Mol Biosci* **5**, 60 (2018).
20. Warfield, R. *et al.* Internally quenched peptides for the study of lysostaphin: an antimicrobial protease that kills Staphylococcus aureus. *Org Biomol Chem* **4**, 3626 (2006).
21. SCHLEIFER, K. H. & FISCHER, U. Description of a New Species of the Genus Staphylococcus: Staphylococcus carnosus. *Int J Syst Bacteriol* **32**, 153–156 (1982).
22. Grabowska, M., Jagielska, E., Czapinska, H., Bochtler, M. & Sabala, I. High resolution structure of an M23 peptidase with a substrate analogue. *Scientific Reports 2015 5:1* **5**, 1–8 (2015).
23. Browder, H. P., Zygmunt, W. A., Young, J. R. & Tavormina, P. A. Lysostaphin: Enzymatic mode of action. *Biochem Biophys Res Commun* **19**, 383–389 (1965).
24. Sloan, G. L., Smith, E. C. & Lancaster, J. H. Lysostaphin endopeptidase-catalysed transpeptidation reactions of the imino-transfer type. *Biochemical Journal* **167**, 293–296 (1977).
25. Schneewind, O., Fowler, A. & Faull, K. F. Structure of the Cell Wall Anchor of Surface Proteins in Staphylococcus aureus. *Science (1979)* **268**, 103–106 (1995).
26. Maya-Martinez, R. *et al.* Recognition of peptidoglycan fragments by the transpeptidase PBP4 from staphylococcus aureus. *Front Microbiol* **10**, 3223 (2019).
27. Xu, N., Huang, Z.-H., de Jonge, B. L. M. & Gage, D. A. Structural Characterization of Peptidoglycan Muropeptides by Matrix-Assisted Laser Desorption Ionization Mass Spectrometry and Postsource Decay Analysis. *Anal Biochem* **248**, 7–14 (1997).
28. Firczuk, M., Mucha, A. & Bochtler, M. Crystal Structures of Active LytM. *J Mol Biol* **354**, 578–590 (2005).
29. Frankel, M. B., Hendrickx, A. P. A., Missiakas, D. M. & Schneewind, O. LytN, a Murein Hydrolase in the Cross-wall Compartment of Staphylococcus aureus, Is Involved in Proper Bacterial Growth and Envelope Assembly. *Journal of Biological Chemistry* **286**, 32593–32605 (2011).
30. Małecki, P. H. *et al.* Structural Characterization of EnpA D,L-Endopeptidase from Enterococcus faecalis Prophage Provides Insights into Substrate Specificity of M23 Peptidases. *Int J Mol Sci* **22**, (2021).
31. Kühner, D., Stahl, M., Demircioglu, D. D. & Bertsche, U. From cells to muropeptide structures in 24 h: Peptidoglycan mapping by UPLC-MS. *Sci Rep* **4**, 1–7 (2014).
32. Gründling, A., Missiakas, D. M. & Schneewind, O. Staphylococcus aureus Mutants with Increased Lysostaphin Resistance. *J Bacteriol* **188**, 6286 (2006).
33. Strandén, A. M., Ehlert, K., Labischinski, H. & Berger-Bächi, B. Cell wall monoglycine cross-bridges and methicillin hypersusceptibility in a femAB null mutant of methicillin-resistant Staphylococcus aureus. *J Bacteriol* **179**, 9–16 (1997).
34. Sugai, M. *et al.* epr, which encodes glycylglycine endopeptidase resistance, is homologous to femAB and affects serine content of peptidoglycan cross bridges in Staphylococcus capitis and Staphylococcus aureus. *J Bacteriol* **179**, 4311–4318 (1997).
35. Thumm, G. & Gotz, F. Studies on prolysostaphin processing and characterization of the lysostaphin immunity factor (Lif) of Staphylococcus simulans biovar staphylolyticus. *Mol Microbiol* **23**, 1251–1255 (1997).
36. Tschierske, M., Ehlert, K., Strandén, A. M. & Berger-Bächi, B. Lif, the lysostaphin immunity factor, complements FemB in staphylococcal peptidoglycan interpeptide bridge formation. *FEMS Microbiol Lett* **153**, 261–264 (2006).
37. Schechter, I. & Berger, A. On the size of the active site in proteases. I. Papain. *Biochem Biophys Res Commun* **27**, 157–162 (1967).

38. Reste de Roca, F. *et al.* Cleavage Specificity of Enterococcus faecalis EnpA (EF1473), a Peptidoglycan Endopeptidase Related to the LytM/Lysostaphin Family of Metallopeptidases. *J Mol Biol* **398**, 507–517 (2010).
39. Sabala, I. *et al.* Crystal structure of the antimicrobial peptidase lysostaphin from Staphylococcus simulans. *FEBS J* **281**, 4112–4122 (2014).
40. Kusuma, C. M. & Kokai-Kun, J. F. Comparison of Four Methods for Determining Lysostaphin Susceptibility of Various Strains of Staphylococcus aureus. *Antimicrob Agents Chemother* **49**, 3256–3263 (2005).
41. Schrödinger 2021-4: Maestro, Schrödinger, LLC, New York (2021).
42. Friesner, R. A. *et al.* Glide: A New Approach for Rapid, Accurate Docking and Scoring. 1. Method and Assessment of Docking Accuracy. *J Med Chem* **47**, 1739–1749 (2004).
43. Halgren, T. A. *et al.* Glide: A New Approach for Rapid, Accurate Docking and Scoring. 2. Enrichment Factors in Database Screening. *J Med Chem* **47**, 1750–1759 (2004).
44. Friesner, R. A. *et al.* Extra Precision Glide: Docking and Scoring Incorporating a Model of Hydrophobic Enclosure for Protein−Ligand Complexes. *J Med Chem* **49**, 6177–6196 (2006).
45. Schrödinger, L. & DeLano, W. PyMOL. (2020).